Geophysical Research Letters

RESEARCH LETTER
10.1029/2022GL100296

Special Section:
The Arctic: An AGU Joint Special Collection

Quantifying Ice-Sheet Derived Lead (Pb) Fluxes to the Ocean; A Case Study at Nioghalvfjerdsbræ

Stephan Krisch[1,2], Oliver Huhn[3], Ali Al-Hashem[1], Mark J. Hopwood[1,4], Pablo Lodeiro[1,5], and Eric P. Achterberg[1]

[1]GEOMAR Helmholtz Centre for Ocean Research Kiel, Kiel, Germany, [2]Now at Federal Institute of Hydrology, Koblenz, Germany, [3]Institute of Environmental Physics, University of Bremen, Bremen, Germany, [4]Department of Ocean Science and Engineering, Southern University of Science and Technology, Shenzhen, China, [5]Department of Chemistry, University of Lleida–AGROTECNIO-CERCA Center, Lleida, Spain

Key Points:

- Helium and neon show strong evidence for a subglacial source of Pb discharging onto the NE Greenland Shelf
- Contrasting inflowing and outflowing waters beneath the floating ice tongue of Nioghalvfjerdsbræ shows a 2-3-fold dPb enrichment
- The dissolved Pb flux from Nioghalvfjerdsbræ (2.2 ± 1.4 Mg·yr^{-1}) is comparable to small Arctic rivers, with ~90% of a sedimentary origin

Supporting Information:

Supporting Information may be found in the online version of this article.

Correspondence to:

S. Krisch and E. P. Achterberg, stephankrisch.sk@gmail.com; eachterberg@geomar.de

Citation:

Krisch, S., Huhn, O., Al-Hashem, A., Hopwood, M. J., Lodeiro, P., & Achterberg, E. P. (2022). Quantifying ice-sheet derived lead (Pb) fluxes to the ocean; a case study at Nioghalvfjerdsbræ. *Geophysical Research Letters*, *49*, e2022GL100296. https://doi.org/10.1029/2022GL100296

Received 4 JUL 2022
Accepted 17 OCT 2022

Author Contributions:

Conceptualization: Stephan Krisch
Formal analysis: Stephan Krisch, Oliver Huhn, Ali Al-Hashem
Funding acquisition: Eric P. Achterberg
Investigation: Stephan Krisch
Methodology: Stephan Krisch

Abstract

Concentrations of the toxic element lead (Pb) are elevated in seawater due to historical emissions. While anthropogenic atmospheric emissions are the dominant source of dissolved Pb (dPb) to the Atlantic Ocean, evidence is emerging of a natural source associated with subglacial discharge into the ocean but this has yet to be constrained around Greenland. Here, we show subglacial discharge from the cavity underneath Nioghalvfjerdsbræ floating ice tongue, is a previously unrecognized source of dPb to the NE Greenland Shelf. Contrasting cavity-inflowing and cavity-outflowing waters, we constrain the associated net-dPb flux as 2.2 ± 1.4 Mg·yr^{-1}, of which ~90% originates from dissolution of glacial bedrock and cavity sediments. We propose that the retreat of the floating ice tongue, the ongoing retreat of many glaciers on Greenland, associated shifts in sediment dynamics, and enhanced meltwater discharges into shelf waters may result in pronounced changes, possibly increases, in net-dPb fluxes to coastal waters.

Plain Language Summary

Lead (Pb) is a toxic element. Hundreds of thousands of tons have historically been emitted into the atmosphere through use of leaded gasoline, ore-smelting and coal-combustion which led to large-scale deposition of Pb into the ocean and onto the Greenland Ice Sheet. Since the phase-out of leaded gasoline, concentrations of dissolved Pb in the surface ocean have declined, increasing the relative importance of other, natural sources of Pb to the marine environment. In 2016, we conducted a survey near Nioghalvfjerdsbræ, one of Greenland's largest marine-terminating glaciers, to investigate if Greenland Ice Sheet discharge is a source of Pb to the Northeast Greenland Shelf. We observed elevated dissolved Pb concentrations at intermediate depths within a ~60 km radius downstream of the Nioghalvfjerdsbræ terminus. The Pb enrichment originates from underneath the glacier's floating ice tongue. Lead sources underneath Nioghalvfjerdsbræ likely include Pb from eroded bedrock and exchange with fjord sediments. Our calculations suggest that Nioghalvfjerdsbræ dissolved Pb discharge is comparable to that from small Arctic rivers. Given the widespread occurance of Pb-rich minerals across Greenland, observed increases in meltwater discharge and the retreat of marine-terminating glaciers could increase dPb supply to Greenlandic shelf regions.

1. Introduction

Lead (Pb) is a toxic element to humans (Carrington et al., 2019; Wani et al., 2015) and accumulation in marine biota a pathway of exposure (Burger et al., 2012; Zimmer et al., 2011). Lead emissions from coal combustion and the use of tetraethyllead as an additive to gasoline through the twentieth century (McConnell & Edwards, 2008; Pacyna & Pacyna, 2001) resulted in large scale atmospheric deposition of anthropogenic Pb across the surface ocean (Boyle et al., 2014). Whilst Pb concentrations across the North Atlantic are now declining, they remain above pre-industrial concentrations (Kelly et al., 2009; Noble et al., 2015). The ultimate fate of Pb in the marine environment is governed by its high affinity to particles (Dewey et al., 2021; Yang et al., 2015), which results in a dissolved Pb (dPb) distribution strongly affected by lateral transfer within sinking matter and burial in sediments (Bruland et al., 2013). However, a growing number of studies have shown intermittent release of dPb from shelf sediments (Cobelo-García & Prego, 2004; Kalnejais et al., 2007; Martino et al., 2002). This suggests that shelf sediments affected by a legacy of anthropogenic Pb deposition may continue to act as a dPb source to the water column (Rusiecka et al., 2018; Vieira et al., 2019).

Project Administration: Eric P. Achterberg
Resources: Eric P. Achterberg
Supervision: Mark J. Hopwood, Eric P. Achterberg
Validation: Stephan Krisch, Oliver Huhn, Ali Al-Hashem, Pablo Lodeiro
Visualization: Stephan Krisch
Writing – original draft: Stephan Krisch
Writing – review & editing: Stephan Krisch, Oliver Huhn, Ali Al-Hashem, Mark J. Hopwood, Pablo Lodeiro, Eric P. Achterberg

Whilst Pb distributions across the North Atlantic (Bacon et al., 1988; Rusiecka et al., 2018) and North Pacific (Chien et al., 2017; Sañudo-Wilhelmy & Flegal, 1994) are now well described, comparatively little is known about the biogeochemical cycling of Pb in the Arctic (Colombo, Rogalla, et al., 2019; de Vera et al., 2021) and high latitude (>65°N) North Atlantic shelf seas (Schlosser & Garbe-Schönberg, 2019). Rivers draining into the Arctic Ocean deliver large quantities of mostly natural Pb to shelf regions (Colombo, Brown, et al., 2019; Guay et al., 2010; Guieu et al., 1996). Whilst under some circumstances large fractions of freshwater dPb are lost from the water column during estuarine mixing (Dai & Martin, 1995; Tanguy et al., 2011), conversely, some conservative behavior of dPb has been observed (Guieu et al., 1996). This may be the result of a complex interplay between aggregation/scavenging and sedimentation of Pb (Balistrieri & Murray, 1984; Waeles et al., 2007; Yang et al., 2015), and dissolution of Pb from sediments and particles following resuspension (Cobelo-García & Prego, 2004; Kalnejais et al., 2007; Martino et al., 2002) or changes in sediment redox chemistry (Benoit & Hemond, 1990; Rivera-Duarte & Flegal, 1994). A similarly complex interplay may affect Pb dynamics from glacier-derived freshwater. A few studies investigating Pb cycling in the vicinity of small glaciers in Svalbard and the Canadian Arctic Archipelago have shown elevated suspended particulate or dissolved Pb concentrations (Bazzano et al., 2017; Colombo, Rogalla, et al., 2019) which could reflect a combination of Pb release from subglacial weathering (Hawkings et al., 2020; Kolb et al., 2016) and anthropogenic Pb contamination embedded in glacial ice and snow (Hong et al., 1994; Sherrell et al., 2000).

Given the potential for an enhanced Pb efflux under future scenarios of continued Greenland Ice Sheet discharge and glacier retreat (Aschwanden et al., 2019; Fahrner et al., 2021), here we present a survey investigating the effects of glacial discharge on downstream Pb distributions from Nioghalvfjerdsbræ (79N Glacier). Nioghalvfjerdsbræ is one of Greenland's largest marine terminating glaciers (Rignot & Mouginot, 2012) accounting for ~2% of 2016 Greenland Ice Sheet runoff and solid ice discharge (Bamber et al., 2018). By combining dissolved, total dissolvable and labile particulate Pb data with helium (He) and neon (Ne) tracers of subglacial meltwater, we demonstrate a sustained release of freshwater and sediment-sourced dPb from Nioghalvfjerdsbræ to the NE Greenland Shelf, and the potential for future changes in Greenland dPb efflux.

2. Methods

2.1. Sampling

Polarstern expedition PS100 (GN05) sampled the NE Greenland Shelf (NEGS) in August 2016 (boreal summer) and was equipped with two CTD rosette systems for water column profiling; an ultraclean CTD system (ucCTD) for contamination-prone parameters, and a large CTD system for other parameters. Twelve ucCTD stations were sampled for trace elements (Pb, Fe, Mn, Co, Ni, Cu, and Zn) and macronutrients (NO_3, PO_4, and $Si(OH)_4$) on the NEGS (>5°W), of which 6 stations were located on the inner shelf region (>15°W) in close proximity to the Nioghalvfjerdsbræ terminus (station 1) (Supplementary Figure S1). Additional stations were sampled for He and Ne with the large CTD system. For water column physical properties (salinity, temperature, pressure, light attenuation ("turbidity"), UV-light fluorescence), the data set from the ucCTD (SEA-BIRD SBE 911) was combined with the large CTD data (SEA-BIRD SBE 911plus). A total of 10 stations sampled the shelf for trace elements and He/Ne, within 1 hr at the same location, providing to our knowledge a unique data set for the investigation of subglacial Pb cycling from a retreating ice shelf.

2.2. Trace Element and Macronutrient Analyses

Trace element samples were collected following GEOTRACES sampling protocols (Cutter et al., 2017) using the powder-coated aluminum ucCTD equipped with 24 × 12 L GoFlo bottles (Ocean Test Equipment) as per Krisch, Hopwood, et al. (2021). For the analyses of dissolved trace elements, samples were filtered (Acropak 0.8/0.2 µm) and acidified to pH 1.9 with HCl (UpA, ROMIL). Unfiltered samples were retained and acidified as above to determine total dissolvable trace elements after >6 months of storage. Particulate trace elements were collected onto pre-acid cleaned Polyethersulfone (PES) membrane filters (0.2 µm, Sartorius). Filters were stored in a deep freezer (−20°C) until analysis. The determination of labile particulate trace elements was conducted following the procedure of Berger et al. (2008), applying a weak acid leach (25% acetic acid, Optima grade, Fisher Scientific) with a mild reducing agent (0.02 M hydroxylamine hydrochloride, Sigma TM grade).

Trace elements in seawater samples were quantified by high-resolution inductively coupled plasma mass spectrometry (HR-ICP-MS, Element-XR, Thermo Fisher Scientific) after matrix-removal and pre-concentration using an automated SeaFAST system (SC-4 DX SeaFAST pico, ESI) as described by Rapp et al. (2017). The analyses of labile particulate trace elements were conducted via HR-ICP-MS (Element-XR, Thermo Fisher Scientific) without preconcentration. Validation of method accuracy for dissolved and total dissolvable trace element analyses was through GEOTRACES SAFe S and GSC reference materials (Bruland Research Lab, 2009) (Tables S1 and S2 in the Supporting Information S1). Particulate analyses and leach consistency between digestion batches were validated using BCR-414 reference material (Joint Research Centre, 2017).

Seawater for macronutrient analyses of NO_3, PO_4 and $Si(OH)_4$ was also retained from each GoFlo rosette bottle and analyzed as described in Krisch et al. (2020). Details on measurement validation can be found with the macronutrient data report (Graeve et al., 2019).

2.3. Noble Gas Measurements (Helium and Neon)

The procedure for sampling and analyses of He (^{3}He, ^{4}He) and Ne (^{20}Ne, ^{22}Ne) stable isotopes during PS100, and subsequent calculation of subglacial meltwater fractions (SMW) in the water column, is described by Huhn, Rhein, Kanzow, et al. (2021). Calculation of SMW follows the method of Rhein et al. (2018) and assumes that He/Ne enrichment in glacial ice is the result of atmospheric gases of constant composition being trapped in the ice matrix and fully dissolved when the glacial ice melts under enhanced hydrostatic pressure. Any additional He in glacial ice is attributed to radioactive α-decay of heavy nuclides in the bedrock ("crustal He") (Huhn et al., 2018; Jean-Baptiste et al., 2001). Please note that drainage of surface melt to the glacier's grounding line and its contribution to freshwater budgets beneath the floating ice tongue is not included in SMW fractions due to equilibration with the atmosphere. The overall uncertainty in He- and Ne-based SMW fractions is 0.1% (Huhn, Rhein, Kanzow, et al., 2021). SMW fractions >0.1% are thus considered significant. Helium- and Ne-based calculations of SMW fractions are identical within 0.1% variance (1σ for all significant SMW fractions). Thus, for a conservative estimate of SMW influence on the shelf, we use the He- or Ne-based SMW fraction that is lowest. He/Ne ratios >2% above the atmospheric ratio are considered to be enriched in He from the bedrock (Huhn, Rhein, Kanzow, et al., 2021).

3. Results and Discussion

3.1. Study Region

Three water masses are present on the NEGS (Schaffer et al., 2017). Polar Surface Water (PSW, $\sigma_\Theta < 26.1$ kg/m^3) is found across the NEGS and its depth range increases from the Greenland continental shelf break (0–20 m at station 8) toward Nioghalvfjerdsbræ and the Greenlandic coast (0–69 m at station 1) (Figure 1). Below the PSW layer, modified Atlantic Intermediate Water (mAIW, $\sigma_\Theta = 27.00 - 27.73$ kg/m^3) forms the bottom water in shallow and central parts of the shelf (stations 3, 12 and 13) and its thickness increases from the outer NEGS (48–158 m at station 8) toward the Greenlandic coast (96–267 m at station 1). Atlantic Intermediate Water (AIW, $\sigma_\Theta > 27.73$ kg/m^3) forms the bottom water in the deeper parts of the NEGS and is found in the C-shaped trough system consisting of Norske Trough (stations 8–10) in the southern parts of the shelf and Westwind Trough (stations 3, 5, and 6) in the northern parts of the shelf.

Bathymetry governs water mass movement across the shelf (Bourke et al., 1987; Schaffer et al., 2017). The East Greenland Current forms the eastern limb of the anti-cyclonic NE Greenland Coastal Circulation and steers cold and low-salinity PSW over the shelf (Bourke et al., 1987). Warm and saline AIW is advected along a trough system toward the Greenlandic coast and the marine-terminating glaciers of the NE Greenland Ice Sheet (Schaffer et al., 2020; Wilson & Straneo, 2015). A sill near station 3 (at 237 m depth) restricts AIW exchange between Norske Trough from Westwind Trough. Only AIW derived via the southern route and Norske Trough may enter the glacial cavity underneath the Nioghalvfjerdsbræ floating ice-tongue through a ~2 km wide inflow depression near station 1 (Schaffer et al., 2017). Advection of PSW (<60 m depth at station 1) underneath the floating ice tongue is restricted by the glacier terminus base, located at ~90 m depth (Schaffer et al., 2020). Following the addition of basal meltwater and subglacial runoff, mAIW exits the glacier cavity at intermediate depth after a residence time of ~162 days (2016 data) (Huhn, Rhein, Kanzow, et al., 2021; Schaffer et al., 2020)

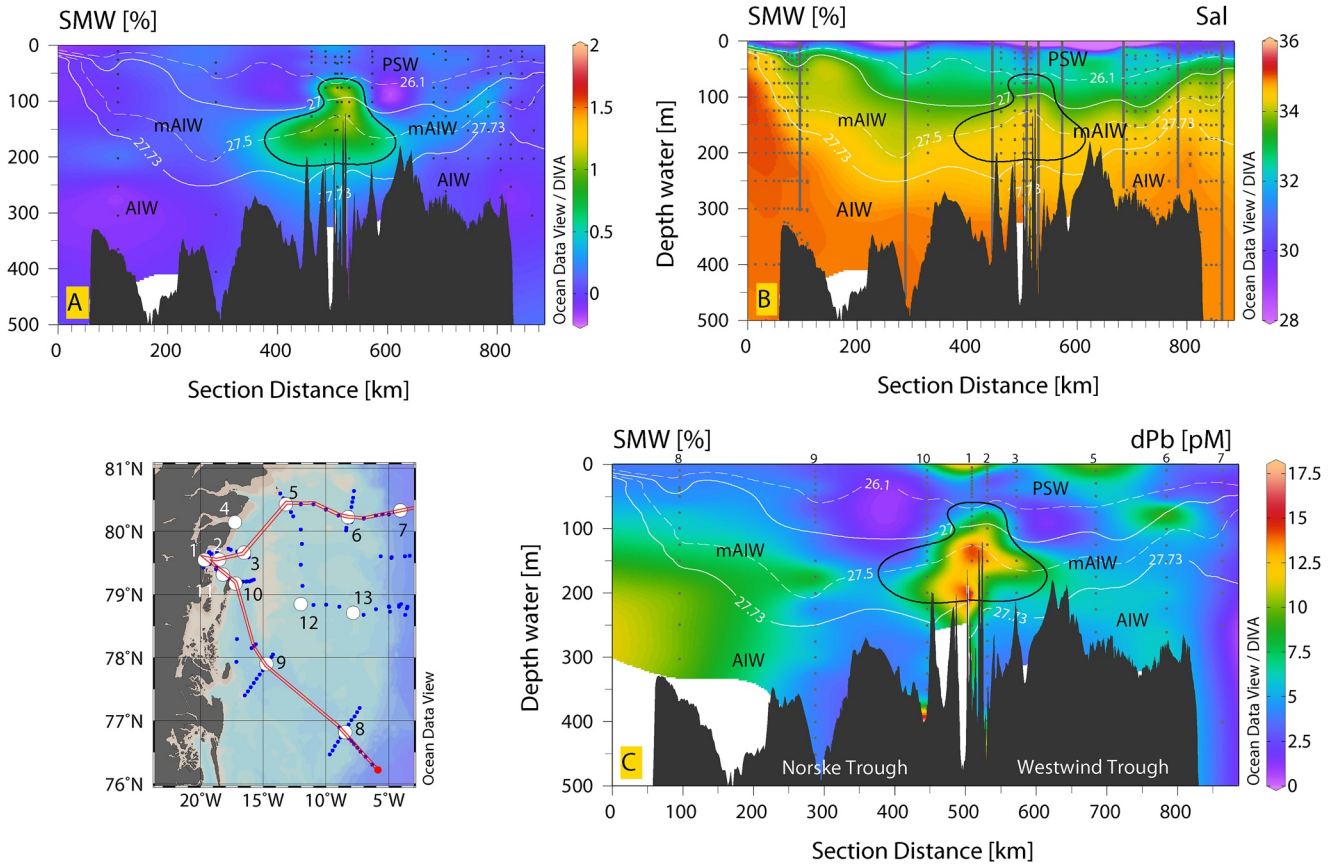

Figure 1. Distribution of (a) subglacial meltwater content (SMW, %), (b) salinity (Sal) and (c) dissolved Pb (dPb, pmol·L^{-1}, pM) overlain with contours of 0.5% SMW (black bold line) on the NE Greenland Shelf. The transect (indicated by red contours in the station map) follows the shelf's C-shaped trough system from Norske Trough (stations 8–10) toward Nioghalvfjerdsbræ terminus (station 1), Westwind Trough (stations 3–6), and Fram Strait (station 7) (Figure S1 in the Supporting Information S1). Isopycnal surfaces (white contours) distinguish between Polar Surface Water (PSW, σ_Θ < 26.1 kg/m^3), Atlantic Intermediate Water (AIW, σ_Θ > 27.73 kg/m^3), and modified AIW (mAIW, σ_Θ = 27.00–27.73 kg/m^3). Black dots indicate depths of discrete CTD measurements and water sampling; vertical lines (bold gray) indicate ultraclean CTD measurements. Ultraclean CTD station numbers are indicated in 'C' and on the station map (bottom left). Depth profiles of dPb for each individual station are shown in Figure S3 in the Supporting Information S1.

and is subsequently advected away from the Nioghalvfjerdsbræ terminus toward the NEGS break (Huhn, Rhein, Kanzow, et al., 2021; Laukert et al., 2017).

3.2. Dissolved Pb Distributions

Concentrations of dPb in the water column on the NEGS (stations 1–6 and 8–13, Figure 1) ranged between 2.0 and 15.9 pmol. L^{-1} (pM hereafter). Dissolved Pb concentrations increased with depth in the southern and outer parts of the shelf in Norske Trough (range: 3.6–10.3 pM at station 8), in contrast to stations on the inner NEGS (e.g., 3.5–15.9 pM at station 1) where pronounced mid-depth maxima were observed (Figures S2 and S3 in the Supporting Information S1). Surface dPb concentrations spanned a similar range on the NEGS (2.7–13.3 pM at 10 m depth) but evidenced local maxima only near the glacier terminus of Nioghalvfjerdsbræ (11.2 pM at 5 m, station 1) and at the Dimphna Sund sill (13.3 pM at 10 m, station 4) (Figure S4 in the Supporting Information S1).

The concentrations of dPb in the water column on the NEGS followed a trend consistent with the general circulation of the region. Surface dPb concentrations near the Greenland continental shelf break (3.5 ± 0.7 pM at <50 m, stations 6, 8 and 13) matched observations from the Transpolar Drift in the Central Arctic (3.5 ± 0.8 pM at <50 m depth (stations 81, 87, 96 and 99 as per Gerringa et al., 2021)) and suggest a strong influence of Arctic Ocean outflow on the distribution of dPb in surface waters of the outer NEGS. A similar trend is also evident in the distribution of many other dissolved trace elements including Fe (dFe), Mn (dMn) and Co (dCo) (Krisch et al., 2022). In contrast, advection of Atlantic Water, enriched in dPb (Schlosser & Garbe-Schönberg, 2019), into

Norske Trough (Schaffer et al., 2017) is likely the main source contributing to elevated dPb concentrations in AIW near the southern shelf break (10.0 ± 0.2 pM at 200–303 m, station 8, Figure 1). There, dPb concentrations were 2-3-fold depleted compared to subsurface Atlantic Water of the Iceland Basin (26.7 ± 3.3 pM at 100–446 m (stations 32–36 as per Zurbrick et al., 2018)). Dissolved Pb concentrations decreased further toward the inner NEGS (6.3 ± 2.9 pM at 251–380 m, station 10) and the cavity inflow depression (5.0 ± 1.1 pM at 226–398 m, station 2), potentially caused by scavenging of dPb onto particles (Balistrieri & Murray, 1984) during AIW transport. Modified AIW in close proximity to Nioghalvfjerdsbræ terminus was the most dPb-enriched water mass on the NEGS (10.4 ± 2.9 pM at stations 1, 2 and 11). Concentrations in mAIW exceeded observations in AIW (5.8 ± 1.7 pM at stations 1, 2 and 11) by a factor of ~2. This dPb enrichment in mAIW relative to AIW and the general trend of decreasing concentrations in mAIW with distance from Nioghalvfjerdsbræ terminus (station 1, 12.2 ± 3.3 pM) toward Norske Trough (6.2 ± 2.0 pM at station 9) and Westwind Trough (5.0 ± 0.6 pM at station 5) strongly suggests a local source of dPb originating underneath the floating ice tongue.

Dissolved Pb shows a strong linear correlation with salinity for PSW at the Nioghalvfjerdsbræ terminus (0.82 R^2 at 5–60 m depth, Figure S5 in the Supporting Information S1), comparable to observations in estuaries elsewhere (Martino et al., 2002; Tanguy et al., 2011). This corroborates surface freshwater discharge from Nioghalvfjerdsbræ as a likely source of dPb to the NEGS. A linear correlation between dPb and salinity was absent in the water column below the PSW layer (0.04 R^2 at 70–464 m). Yet, elevated dPb concentrations in cavity-exiting mAIW (14.8 ± 0.9 pM at 125–200 m) grouped at slightly lower salinities (34.463 ± 0.078) compared to dPb in cavity-entering AIW (7.5 ± 1.3 pM at salinity of 34.700 ± 0.062 and 300–464 m depth). This suggests that processes beneath the floating ice tongue are also a net source of dPb to the NEGS. Our findings of glacial dPb enrichment in surface and subglacial discharge from Nioghalvfjerdsbræ are in agreement with observations of ~3-fold increases in dPb caused by the addition of glacial meltwater to shelf surface water in Marian Cove on the Antarctic Peninsula (Kim et al., 2015) and elevated dPb concentrations in the Amundsen Sea downstream to the Getz and Dotson Ice Shelfs (Ndungu et al., 2016). Elevated concentrations of dPb in mAIW at all stations on the inner NEGS (7.2 ± 1.4 pM at stations 1–3 and 10–11) (Figure 1) suggest substantial offshore transport of subglacial dPb from Nioghalvfjerdsbræ.

3.3. Subglacial Pb Discharge

Subglacial meltwater discharge can be traced through the use of He and Ne isotopes (Loose & Jenkins, 2014; Rhein et al., 2018). Upon melting of glacial ice, He and Ne are fully dissolved resulting in oversaturation and providing an unambiguous tracer of subsurface water masses affected by subglacial discharge (Huhn et al., 2018; Rhein et al., 2018). The distribution of subglacial meltwater was remarkably similar to the distribution of dPb in the water column on the inner NEGS (Figure 1) and confirms dPb maxima in mAIW downstream of the Nioghalvfjerdsbræ terminus to be subglacial in origin. A weak linear correlation between subglacial meltwater content and dPb concentrations was observed in the water column on the shelf (0.48 R^2, $p < 0.05$, Supplementary Figure S6) which may suggest other factors, besides subglacial meltwater addition, moderate dPb discharge to the shelf. Given the high affinity of dPb for particle surfaces (Dewey et al., 2021; Yang et al., 2015), such factors likely include suspended sediment dynamics (Benoit & Rozan, 1999) underneath the ice tongue.

We conducted a Principal Component Analysis (PCA) to investigate regional relationships between dPb and other water column properties near Nioghalvfjerdsbræ (Figure 2a). The PCA included (a) dPb, dFe, dMn and dCo, (b) nitrate, phosphate and silicic acid, (c) excess He, excess Ne and subglacial meltwater contents, and (d) CTD measurements for depth, salinity and turbidity (i.e., light attenuation). We further included labile particulate and total dissolvable fractions of the trace elements Pb (LpPb, TdPb), Fe (LpFe, TdFe), Mn (LpMn, TdMn) and Co (LpCo, TdCo) in the PCA, referring to reactive particulate trace elements physically immobilized on particles (labile particulates, e.g., Berger et al., 2008), and dissolved and particulate trace elements released after storage under acidic conditions (total dissolvable fraction, e.g., Edwards & Sedwick, 2001). The first two principal components reflect 44.5% (PC1) and 22.4% (PC2) of variance in parameters. In the PCA, dPb grouped with LpPb, TdPb, LpFe, and TdFe and clustered in opposition to light attenuation suggesting a strong influence from particles controlling the distribution of these elements on the inner NEGS. All Pb phases showed a correlation with depth, salinity, and the macronutrients nitrate, phosphate and silicic acid, indicative of influences from depth-dependent processes which may include particle release, scavenging and organic matter remineralization. In contrast, dFe, dMn and dCo grouped with excess He, excess Ne and subglacial meltwater content and showed

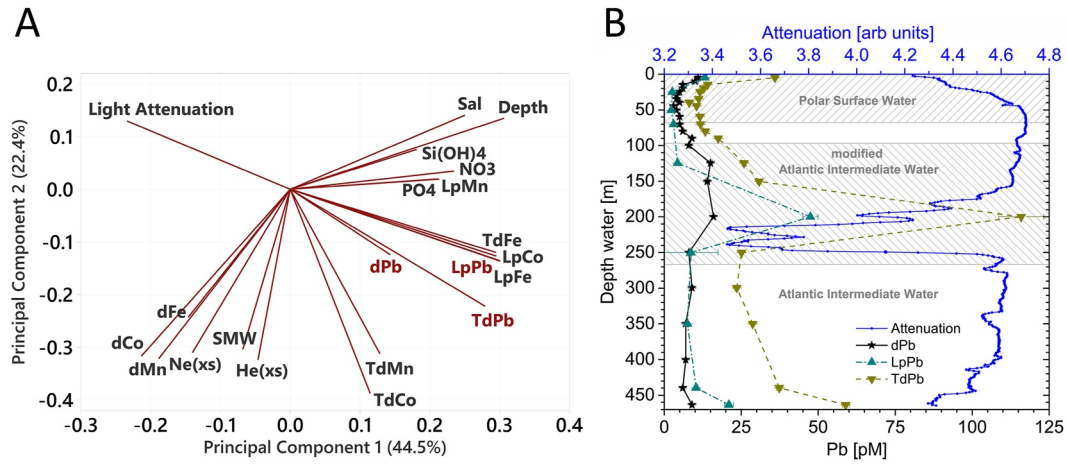

Figure 2. Principal Component Analysis (PCA) and depth profiles of Pb near the Nioghalvfjerdsbræ terminus. (a) The PCA loading plot illustrates trends in the distribution of dissolved, total dissolvable and labile particulate trace elements, and macronutrients, relative to depth, salinity, light attenuation, excess He, excess Ne and subglacial meltwater content (SMW) in the water column on the inner NE Greenland Shelf (stations 1–3 and 10–11). (b) Depth profiles of Pb at the Nioghalvfjerdsbræ terminus (station 1). Dissolved Pb (dPb, black stars), labile particulate Pb (LpPb, blue-green upward triangles), total dissolvable Pb (TdPb, dark-yellow downward triangles) and light attenuation (i.e., turbidity, blue dots). Concentrations of all Pb fractions are in pmol·L^{-1} (pM).

no correlation with respect to their labile and particulate forms and Pb phases. This suggests subglacial meltwater as a source of dFe, dMn and dCo to the inner shelf region and a different supply mechanism for Pb which does not resemble that of the other trace elements.

The distribution of dPb in the water column at the glacier terminus correlated strongly with the distribution of LpPb and TdPb and showed an inverse relationship with light attenuation (Figure 2b) suggesting particles to be a source of particulate and dissolved phases of Pb. Pronounced Pb maxima in mAIW at 125–200 m depth (14.8 ± 0.9 pM dPb, 25.9 ± 21.6 pM LpPb, and 57.5 ± 41.3 pM TdPb) coincided with minima in light attenuation between 150 and 250 m. This is indicative of a particle-rich layer exiting the glacier cavity and speaks out for the importance of a subglacial particle pool in moderating dPb discharge. This is supported by increases in dPb, LpPb and TdPb, and light attenuation minima also near the sediment-bottom water interface. Similar observations have been made in temperate river estuaries (Cobelo-García & Prego, 2004; Waeles et al., 2007). For example, in the Mersey Estuary (United Kingdom) dPb concentration maxima in the upper parts of the estuary coincided with minima in light attenuation suggesting sediment resuspension may be an important factor contributing to water column dPb enrichment (Martino et al., 2002). Our observations of dPb enrichment from sediment Pb sources are in agreement with findings from South Georgia (Southern Ocean) where dPb maxima (46 pM) and LpPb maxima (320 pM, calculated by subtraction of dPb from TdPb) on the shelf were attributed to sediment supply from upstream glaciers (Schlosser & Garbe-Schönberg, 2019).

The strong correlation in the distributions of dPb, LpPb, and TdPb at Nioghalvfjerdsbræ terminus, which is also evident from the PCA analysis (Figure 2a), clearly indicates that subglacial dPb enrichment is caused by addition from a "reactive" pool of Pb underneath the floating ice tongue. Lead dissolution from a reactive, likely sediment-sourced, pool of Pb is also apparent at the entrance sill to Dijmphna Sund (station 4) that functions as a side-exit for Nioghalvfjerdsbræ subglacial discharge into the northern parts of the shelf (Wilson & Straneo, 2015). There, increasing dPb concentrations were observed at enhanced levels of TdPb (0.95 R^2) and correlated with diminished light attenuation throughout the water column (Figures S7 and S8 in the Supporting Information S1). This distribution is similar to observations of dPb enrichment from LpPb and particulate Pb (pPb) on the Celtic Shelf Sea bordering the NE Atlantic Ocean (0.97 R^2 for dPb/LpPb and dPb/pPb at stations C03 and C04, Rusiecka et al., 2018). Such a distribution suggests that increases in reactive Pb (e.g., LpPb) supply underneath the Nioghalvfjerdsbræ ice tongue may result in elevated subglacial dPb export to the NEGS. However, near the Nioghalvfjerdsbræ terminus (stations 1 and 2), only a weak correlation was observed between dPb/LpPb (0.32 R^2) and dPb/TdPb (0.45 R^2) (Figure S9 in the Supporting Information S1) suggesting some degree of decoupling between dPb and LpPb/TdPb underneath the floating ice tongue. This could arise from a

buffering effect whereby particles are a source of dPb but may also serve as nucleus for dPb scavenging, making net dPb release very sensitive to the suspended sediment load (Balls, 1989; Benoit, 1995). A similar phenomenon affects the relationship between dissolved and particulate Fe phases in a broad range of contexts (Homoky et al., 2012; Wagener et al., 2010).

The comparatively constant dPb concentrations at the glacier terminus between 125 and 200 m depth (14.8 ± 0.9 pM), even at 200 m where pronounced peaks in LpPb, TdPb and turbidity were observed (Figure 2b), together with only weak correlations between dPb and LpPb/TdPb near the glacier terminus (Figure S9 in the Supporting Information S1), does suggest a near-steady state between dPb dissolution, and (re-)adsorption/scavenging in cavity-exiting mAIW. The extended cavity residence time of waters underneath the floating ice tongue of several months to a year (Schaffer et al., 2020; Wilson & Straneo, 2015) may have aided the establishment of such a steady state system. A similar mechanism has been proposed to moderate subglacial dFe discharge from Nioghalvfjerdsbræ (Krisch, Hopwood, et al., 2021) and several studies in a global context have suggested the existence of a "dynamic equilibrium" between dissolution and (re-)adsorption/scavenging of dPb onto particles (Rusiecka et al., 2018; Schlosser & Garbe-Schönberg, 2019; Sherrell et al., 1992). This raises questions concerning how ongoing ice shelf retreat may affect net-dPb release. The subsurface lateral export of dPb in mAIW might be diminished if lateral transport occurred in surface waters (instead of subsurface waters) where particle scavenging and biological dPb uptake (Fisher et al., 1987; Santana-Casiano et al., 1995; Tanaka et al., 1983) is likely more severe. On the other hand, shifts in circulation and suspended sediment load dynamics may be the major control on local dPb concentrations, and more rapid discharge of cavity waters including entrained sediments may overall increase subglacial dPb export.

3.4. Is Glacial Bedrock a Source of dPb?

Pb-rich minerals in cavity sediments and overridden bedrock are likely contributing to the ~3-fold increase in dPb between cavity-entering AIW (5.0 ± 1.1 pM at station 2) and subglacial mAIW discharge (14.8 ± 0.9 pM between 125 and 200 m depth, station 1) to the NEGS. Extensive Pb-rich deposits have been found in Western and Northern Greenland (Kolb et al., 2016) including Citronen Fjord ~200 km north of Nioghalvfjerdsfjorden where the content of Pb in minerals reaches ~1% (Kragh et al., 1997). The widespread nature of Pb-rich deposits in Northern Greenland suggests that the NE Greenland Ice Sheet may be eroding bedrock with an enhanced Pb content relative to the crustal mean. Weathering of polymetallic deposits, including galena (PbS), would increase the solubility of Pb (Lara et al., 2011) underneath the ice sheet and thus may result in enrichment of glacial meltwater with dPb.

On the NEGS, excluding observations between 75 and 125 m near Nioghalvfjerdsbræ and Zachariæ Isstrøm (stations 1, 2 and 11), a strong correlation between crustal He and water column dPb concentrations was observed (0.89 R^2, Figure S6 in the Supporting Information S1) suggesting that dPb enrichment in shelf water may stem from dissolution of bedrock. A similar trend, however off-set to elevated crustal He concentrations, at 75–125 m downstream to Nioghalvfjerdsbræ and Zachariæ Isstrøm (0.95 R^2 at stations 1, 2 and 11) is potentially caused by crustal He diffusion into upper layers of glacial ice (Jean-Baptiste et al., 2001) and subsequent enrichment of meltwater with crustal He but comparatively minor quantities of dPb. Alternatively, more efficient scavenging of dPb in sub-surface waters may explain this deviating trend downstream to the glacier termini of Nioghalvfjerdsbræ and Zachariæ Isstrøm.

Dissolution of Pb from bedrock and shelf sediments, and scavenging of dPb downstream to Nioghalvfjerdsbræ, seems to be coupled to the cycling of Fe which is present at much higher concentrations in dissolved and particulate phases (Krisch, Hopwood, et al., 2021). Dissolution of Fe carrier phases, for example, under sub- or anoxic conditions (Dewey et al., 2021; Herbert et al., 2020), can liberate dPb into sediment poor waters (Kalnejais et al., 2015; Rivera-Duarte & Flegal, 1994) and, aided by resuspension, may enhance dPb concentrations in shelf bottom waters (Ferrari & Ferrario, 1989; Rusiecka et al., 2018). Conversely, Fe-oxide formation can be important for Pb scavenging (Filipek et al., 1981; Waeles et al., 2007) and thus, may be efficient shuttles for Pb sedimentation (Wei & Murray, 1994; Yang et al., 2015). Downstream to the Nioghalvfjerdsbræ terminus, a strong correlation was observed for dPb and dFe in cavity-exiting mAIW on the inner shelf region (0.70 R^2 for stations 1–3 and 10–11, Figure S10 in the Supporting Information S1) suggesting a dependency of subglacial dPb enrichment on the dissolution of Fe carrier phases similar to temperate estuaries such as the Penzé estuary (France, 0.87 R^2, Tanguy et al., 2011). The strong correlation of dPb with dFe also suggests that pronounced decreases

during offshore dPb transport in mAIW from the Nioghalvfjerdsbræ terminus (12.2 ± 3.3 pM at station 1) toward Westwind Trough (5.0 ± 0.6 pM at station 5) may be linked to scavenging with dFe, although there is likely also dilution with dPb- and dFe-depleted waters from upstream to the anticyclonic coastal circulation. The absence of a correlation between dPb and dMn in mAIW on the inner NEGS (0.15 R^2) is indicative of limited influence from Mn phases on the distribution of dPb downstream to Nioghalvfjerdsbræ which is in agreement with the observations of Filipek et al. (1981) suggesting comparatively weak competition of Mn-oxides in the scavenging of Pb relative to Fe-oxides. Unfortunately, there are no other glacial systems, to our knowledge, where outflow of modified cavity waters and it's Pb and Fe concentrations have been constrained at a similar resolution and thus it is unclear to what extent these processes are representative of other systems on a global scale. The similarities with temperate estuaries do however at least suggest that glacier outflows exhibit similar mechanistic processes as lower latitude systems.

3.5. Dissolved Pb Flux Calculations

Nioghalvfjerdsbræ is an ideal location for investigations into glacial trace element cycling. Nioghalvfjerdsbræ is one of Greenland's largest marine-terminating glaciers and drains ∼6% of the Greenland Ice Sheet by area (Rignot & Mouginot, 2012). The circulation on the NEGS is well constrained (Bourke et al., 1987; Schaffer et al., 2017) and so are the processes controlling water exchange between the shelf and the subglacial cavity (Schaffer et al., 2020; Wilson & Straneo, 2015). While surface runoff around Greenland follows a seasonal cycle with maximum discharge expected to occur in late summer (e.g., Mortensen et al., 2013), basal melting which contributes ∼80% to the non-calving mass loss from Nioghalvfjerdsbræ (Wilson et al., 2017) occurs throughout the year and shows minor seasonal variability (Schaffer et al., 2020).

For the calculation of subglacial dPb export from Nioghalvfjerdsbræ, we apply the approach outlined in Krisch, Hopwood, et al. (2021) contrasting the dPb concentration in AIW inflow with mAIW outflow and using the cavity overturning rate derived in the same year as trace metal observations (Schaffer et al., 2020). Contrasting properties of dPb in cavity-exiting mAIW (12.2 ± 3.3 pM at station 1) relative to cavity-entering AIW (5.0 ± 1.1 pM at station 2) suggests enrichment of 7.2 ± 4.4 pM dPb from freshwater and sediments. Using this difference in dPb load multiplied by the mean cavity volume overturning rate (46 ± 11 mSv, Schaffer et al., 2020) produces a subglacial dPb export flux of 2.2 ± 1.4 $Mg \cdot yr^{-1}$ from Nioghalvfjerdsbræ to the adjacent shelf region.

The total freshwater flux underneath the floating ice tongue from basal melt including subglacial runoff to the grounding line is 0.63 ± 0.21 mSv and contributes 1.4% to the cavity overturning circulation (Schaffer et al., 2020). Melting of pre-industrial ice at the glacier's base (Andersen et al., 2006) and intrusion of surface meltwater to the glacier's base (Das et al., 2008; Young et al., 2022) are likely major contributors to this cavity freshwater flux. To estimate the contribution from the cavity freshwater flux to subglacial dPb discharge, we extrapolate from the dPb-salinity relationship in PSW at the glacier terminus (station 1) to a glacial freshwater endmember of 54 ± 7 pM dPb (at salinity of 0, Figure S5 in the Supporting Information S1). Although the dPb-salinity relationship is not necessarily linear below salinities of 25 (Martino et al., 2002; Waeles et al., 2008) because of non-conservative addition of dPb (e.g., Ferrari & Ferrario, 1989) or non-conservative removal of dPb (e.g., Tanguy et al., 2011) during estuarine mixing, our glacial freshwater endmember is within the broad range of measured pre-industrial Pb levels in Central Greenlandic ice (3.4–73.9 $pmol \cdot kg^{-1}$ for ice core dates of 1236 BC–800 AD, McConnell et al., 2018) and comparable to dPb concentrations in recent Arctic snow deposition sampled in 2015 (48 ± 38 pM as per Marsay, Aguilar-Islas, et al., 2018). The cavity freshwater flux multiplied by the glacial dPb endmember suggests that 0.22 ± 0.08 $Mg \cdot yr^{-1}$, or ∼10% of the subglacial dPb export flux, may stem from the addition of Pb from subglacial runoff and basal melt. In other words, the sedimentary source of dPb is by far the major contribution to dPb exiting the cavity.

The same approach is applied to estimate surface dPb discharge from the Nioghalvfjerdsbræ terminus. The surface meltwater flux from Nioghalvfjerdsbræ has been modeled as 2.3 ± 1.3 $km^3 \cdot yr^{-1}$ (Wilson et al., 2017). We assume this surface meltwater flux to be entirely discharged into the adjacent PSW to obtain an upper limit estimate on surface dPb discharge from the terminus. The surface meltwater flux, multiplied by our glacial dPb endmember, produces an estimate of surface dPb discharge of 0.03 ± 0.01 $Mg \cdot yr^{-1}$ and is thus likely a very minor component (∼1%) in Nioghalvfjerdsbræ dPb export.

Combined, surface meltwater discharge and subglacial freshwater addition may contribute ~11% to the Nioghalvfjerdsbræ dPb export flux of 2.2 ± 1.4 Mg·yr^{-1} with the remaining fraction likely originating from glacial bedrock and cavity sediments. In total, Nioghalvfjerdsbræ dPb export is roughly comparable to dPb discharge from small Arctic rivers such as the Onega River (1.1 ± 0.6 Mg·yr^{-1}) and the Mezen River (1.1 ± 0.6 Mg·yr^{-1}) – though for comparative purposes it should be noted that these fluxes exclude estuarine loss or addition processes (Table S3 in the Supporting Information S1).

4. Conclusion and Future Perspectives

This study demonstrates that Greenland Ice Sheet discharge is a previously unrecognized but important source of dPb to the NEGS. By defining a flux gateway at the glacier terminus, our estimate of Nioghalvfjerdsbræ dPb export (2.2 ± 1.4 Mg·yr^{-1}) is comparable to dPb discharge from small Arctic rivers. The distribution of dPb at Nioghalvfjerdsbræ and the flux calculations suggest that the vast majority of this net dPb export to the shelf, ~90%, is sedimentary in origin. This finding, in the light of widespread occurance of Pb-rich deposits (Kolb et al., 2016; Kragh et al., 1997) and legacy Pb stored in Greenlandic glacial ice and snow (Hong et al., 1994; McConnell & Edwards, 2008; Sherrell et al., 2000), in combination with evidence of glacial Pb supply elsewhere in the Arctic (Bazzano et al., 2017; Hawkings et al., 2020) suggests that most Greenlandic shelf regions are likely receiving dPb inputs from surface and subglacial discharge.

For large marine-terminating glaciers, surface discharge from legacy dPb in glacial ice and snow may only be a minor fraction compared to subglacial dPb discharge which can include larger contributions from sediments and the glacial bedrock. Our calculations suggest that the vast majority of dPb export from Nioghalvfjerdsbræ (~99%) is through subglacial discharge from underneath the floating ice tongue of which only a minor fraction (~10%) stems from the addition of dPb with basal meltwater and subglacial runoff. A long cavity residence time of waters underneath large floating ice tongues or ice shelfs likely results in an equilibration state being approached between dissolved and particulate fractions of Pb. Consequently, the retreat of large marine-terminating glaciers and more rapid release of cavity waters to the shelf may drive more dynamic and variable subglacial dPb export to coastal regions.

Our observations suggest that sediment dynamics are likely the most important factor controlling glacial dPb release into the marine environment. In the context of glacier retreat, increasing sediment delivery to the marine environment (Chu et al., 2012; Hudson et al., 2014) has the potential to increase dPb export into near-shore surface waters. However, rapid scavenging of dPb and onto particles (Marani et al., 1995; Tanguy et al., 2011; Yang et al., 2015) as indicated by the succinct decline in dPb concentrations with distance from Nioghalvfjerdsbræ terminus (Figure 1, Figure S9 in the Supporting Information S1) is likely to limit long-distance dPb transport. Future increases in surface and subglacial dPb export may thus predominantly affect inner shelf regions with rapidly decreasing glacial dPb fluxes with distance from the terminus. Nevertheless, the existence of a dynamic equilibrium between dPb scavenging and release (Rusiecka et al., 2018; Sherrell et al., 1992) in conjunction with net dissolution of dPb following resuspension of sediments (Figure 2, Figure S8 in the Supporting Information S1) suggests that scavenged and particle-bound labile Pb may continue to function as a source of dPb beyond coastal NE Greenland.

Conflict of Interest

The authors declare no conflicts of interest relevant to this study.

Data Availability Statement

All data used throughout this publication is accessible online. Physical oceanography data can be obtained from: https://doi.pangaea.de/10.1594/PANGAEA.871028 (large CTD, Kanzow et al., 2017), and https://doi.pangaea.de/10.1594/PANGAEA.871030 (ucCTD, Kanzow et al., 2017). Macronutrient data can be obtained from: https://doi.pangaea.de/10.1594/PANGAEA.879197 (large CTD, Graeve & Ludwichowski, 2017), and https://doi.pangaea.de/10.1594/PANGAEA.905347 (ucCTD, Graeve et al., 2019). Trace element data can be obtained from: https://doi.pangaea.de/10.1594/PANGAEA.933431 (dissolved trace elements, Krisch, Roig, et al., 2021), and from the source data file of Krisch, Hopwood, et al. (2021) (labile particulate and total dissolvable trace

elements). Helium and Neon data can be obtained from: https://doi.pangaea.de/10.1594/PANGAEA.931336 (Huhn, Rhein, Bulsiewicz, et al., 2021). The section plots (Figure 1) were made using Ocean Data View software with DIVA gridding calculations (Schlitzer, 2022) and RTopo-2.0.1 bedrock topography (30-arc s resolution) (Schaffer et al., 2016). The Principal Component Analysis (Figure 2a) was conducted using Minitab statistical software version 21.1 (Minitab Inc., State College, PA, USA). The depth profiles (Figure 2b) were plotted using OriginPro version 9.1.0. (OriginLab Corporation, Northampton, MA, USA).

Acknowledgments
The authors thank the captain and crew of the RV Polarstern GN05 cruise, operated by the Alfred Wegener Institute, Helmholtz Centre for Polar and Marine Research (AWI). The authors also like to thank Michiel Rutgers van der Loeff (AWI) for his advice upon sampling and ship time management, Takamasa Tsubouchi (University of Bergen, Norway) for the CTD control and Martin Graeve and Kai-Uwe Ludwichowski (both AWI) who performed the macronutrient analyses. The authors are grateful for the help received from Janin Schaffer (AWI), Florian Evers (GEOMAR), Eike Köhn (GEOMAR), Nat Wilson (Woods Hole Oceanographic Institution), and Gerd Rohardt (AWI) for CTD handling and processing, to Nicola Herzberg, Jaw Chuen Yong for assistance during sampling, and to Tim Steffens (all GEOMAR) for technical assistance during HR-ICP-MS analyses. Manuel Colombo (WHOI) is thanked for detailed feedback on this manuscript. Stephan Krisch was financed by GEOMAR and the German Research Foundation (DFG award number AC 217/1-1 to Eric. P. Achterberg). Oliver Huhn was partly funded by the DFG within the Priority Program SPP 1889 "Regional Sea Level and Society" (grants RH25/43 and HU 1544/7) and by the German Federal Ministry of Education and Research (BMBF) within the GROCE project (grant 0F3F0778D). Ali Al-Hashem was financed by the Kuwait Institute for Scientific Research. Mark J. Hopwood was financed by the DFG (award number HO 6321/1-1) and from the GLACE project, organised by the Swiss Polar Institute and supported by the Swiss Polar Foundation. Open Access funding enabled and organized by Projekt DEAL.

References

Andersen, K. K., Svensson, A., Johnsen, S. J., Rasmussen, S. O., Bigler, M., Röthlisberger, R., et al. (2006). The Greenland ice core chronology 2005, 15–42 ka. Part 1: Constructing the time scale. *Quaternary Science Reviews*, *25*, 3246–3257. https://doi.org/10.1016/j.quascirev.2006.08.002

Aschwanden, A., Fahnestock, M. A., Truffer, M., Brinkerhoff, D. J., Hock, R., Khroulev, C., et al. (2019). Contribution of the Greenland Ice Sheet to sea level over the next millennium. *Science Advances*, *5*(6), eaav9396. https://doi.org/10.1126/sciadv.aav9396

Bacon, M. P., Belastock, R. A., Tecotzky, M., Turekian, K. K., & Spencer, D. W. (1988). Lead-210 and polonium-210 in ocean water profiles of the continental shelf and slope south of New England. *Continental Shelf Research*, *8*(5–7), 841–853. https://doi.org/10.1016/0278-4343(88)90079-9

Balistrieri, L. S., & Murray, J. W. (1984). Marine scavenging: Trace metal adsorption by interfacial sediment from MANOP Site H. *Geochimica et Cosmochimica Acta*, *48*(5), 921–929. https://doi.org/10.1016/0016-7037(84)90185-6

Balls, P. W. (1989). The partition of trace metals between dissolved and particulate phases in European coastal waters: A compilation of field data and comparison with laboratory studies. *Netherlands Journal of Sea Research*, *23*(1), 7–14. https://doi.org/10.1016/0077-7579(89)90037-9

Bamber, J. L., Tedstone, A. J., King, M. D., Howat, I. M., Enderlin, E. M., Van den Broeke, M. R., & Noel, B. (2018). Land ice freshwater budget of the Arctic and North Atlantic Oceans: 1. Data, methods, and results. *Journal of Geophysical Research: Oceans*, *123*(3), 1827–1837. https://doi.org/10.1002/2017JC013605

Bazzano, A., Ardini, F., Terol, A., Rivaro, P., Soggia, F., & Grotti, M. (2017). Effects of the Atlantic water and glacial run-off on the spatial distribution of particulate trace elements in the Kongsfjorden. *Marine Chemistry*, *191*, 16–23. https://doi.org/10.1016/j.marchem.2017.02.007

Benoit, G. (1995). Evidence of the particle concentration effect for lead and other metals in fresh waters based on ultraclean technique analyses. *Geochimica et Cosmochimica Acta*, *59*(13), 2677–2687. https://doi.org/10.1016/0016-7037(95)00164-U

Benoit, G., & Hemond, H. F. (1990). 210Po and 210Pb remobilization from lake sediments in relation to iron and manganese cycling. *Environmental Science and Technology*, *24*(8), 1224–1234. https://doi.org/10.1021/es00078a010

Benoit, G., & Rozan, T. F. (1999). The influence of size distribution on the particle concentration effect and trace metal partitioning in rivers. *Geochimica et Cosmochimica Acta*, *63*(1), 113–127. https://doi.org/10.1016/S0016-7037(98)00276-2

Berger, C. J. M., Lippiatt, S. M., Lawrence, M. G., & Bruland, K. W. (2008). Application of a chemical leach technique for estimating labile particulate aluminum, iron, and manganese in the Columbia River plume and coastal waters off Oregon and Washington. *Journal of Geophysical Research*, *113*, C00B01. https://doi.org/10.1029/2007JC004703

Bourke, H., Newton, J. L., Paquette, G., & Tunnicliffe, M. D. (1987). Circulation and water masses of the East Greenland Shelf. *Journal of Geophysical Research*, *92*(C7), 6729–6740. https://doi.org/10.1029/JC092iC07p06729

Boyle, E. A., Lee, J. M., Echegoyen, Y., Noble, A., Moos, S., Carrasco, G., et al. (2014). Anthropogenic lead emissions in the ocean: The evolving global experiment. *Oceanography*, *27*(1), 69–75. https://doi.org/10.5670/oceanog.2014.10

Bruland, K. W., Middag, R., & Lohan, M. C. (2013). *Controls of trace metals in seawater. Treatise on geochemistry: Second edition* (Vol. 8). Elsevier Ltd. https://doi.org/10.1016/B978-0-08-095975-7.00602-1

Bruland Research Lab. (2009). Consensus values for the GEOTRACES 2008 and SAFe reference samples. Retrieved March 12, 2019, from https://websites.pmc.ucsc.edu/~kbruland/GeotracesSaFe/kwbGeotracesSaFe.html

Burger, J., Gochfeld, M., Jeitner, C., Donio, M., & Pittfield, T. (2012). Lead (Pb) in biota and perceptions of Pb exposure at a recently designated superfund beach site in New Jersey. *Journal of Toxicology and Environmental Health Part A: Current Issues*, *75*(5), 272–287. https://doi.org/10.1080/15287394.2012.652058

Carrington, C., Devleesschauwer, B., Gibb, H. J., & Bolger, P. M. (2019). Global burden of intellectual disability resulting from dietary exposure to lead, 2015. *Environmental Research*, *172*, 420–429. https://doi.org/10.1016/j.envres.2019.02.023

Chien, C. Te., Ho, T. Y., Sanborn, M. E., Yin, Q. Z., & Paytan, A. (2017). Lead concentrations and isotopic compositions in the western Philippine Sea. *Marine Chemistry*, *189*, 10–16. https://doi.org/10.1016/j.marchem.2016.12.007

Chu, V. W., Smith, L. C., Rennermalm, A. K., Forster, R. R., & Box, J. E. (2012). Hydrologic controls on coastal suspended sediment plumes around the Greenland Ice Sheet. *The Cryosphere*, *6*(1), 1–19. https://doi.org/10.5194/tc-6-1-2012

Cobelo-García, A., & Prego, R. (2004). Chemical speciation of dissolved copper, lead and zinc in a ria coastal system: The role of resuspended sediments. *Analytica Chimica Acta*, *524*, 109–114. https://doi.org/10.1016/j.aca.2004.05.085

Colombo, M., Brown, K. A., Vera, J. De., Bergquist, B. A., & Orians, K. J. (2019). Trace metal geochemistry of remote rivers in the Canadian Arctic Archipelago. *Chemical Geology*, *525*, 479–491. https://doi.org/10.1016/j.chemgeo.2019.08.006

Colombo, M., Rogalla, B., Myers, P. G., Allen, S. E., & Orians, K. J. (2019). Tracing dissolved lead sources in the Canadian Arctic: Insights from the Canadian GEOTRACES program. *ACS Earth and Space Chemistry*, *3*(7), 1302–1314. https://doi.org/10.1021/acsearthspacechem.9b00083

Cutter, G., Casciotti, K., Croot, P., Geibert, W., Heimbürger, L.-E., Lohan, M., et al. (2017). *Sampling and sample-handling protocols for GEOTRACES cruises*. GEOTRACES Standards and Intercalibration Committee. Retrieved from http://www.geotraces.org/science/intercalibration/222-sampling-and-sample-handling-protocols-for-geotraces-cruises

Dai, M. H., & Martin, J. M. (1995). First data on trace metal level and behaviour in two major Arctic river-estuarine systems (Ob and Yenisey) and in the adjacent Kara Sea, Russia. *Earth and Planetary Science Letters*, *131*(3–4), 127–141. https://doi.org/10.1016/0012-821X(95)00021-4

Das, S. B., Joughin, I., Behn, M. D., Howat, I. M., King, M. A., Lizarralde, D., & Bhatia, M. P. (2008). Fracture propagation to the base of the Greenland ice sheet during supraglacial lake drainage. *Science*, *320*(5877), 778–781. https://doi.org/10.1126/science.1153360

De Vera, J., Chandan, P., Pinedo-González, P., John, S. G., Jackson, S. L., Cullen, J. T., et al. (2021). Anthropogenic lead pervasive in Canadian Arctic seawater. *Proceedings of the National Academy of Sciences of the United States of America*, *118*(24), e2100023118. https://doi.org/10.1073/pnas.2100023118

Dewey, C., Bargar, J. R., & Fendorf, S. (2021). Porewater lead concentrations limited by particulate organic matter coupled with ephemeral iron (III) and sulfide phases during redox cycles within contaminated floodplain soils. *Environmental Science and Technology*, *55*(9), 5878–5886. https://doi.org/10.1021/acs.est.0c08162

Edwards, R., & Sedwick, P. (2001). Iron in East Antarctic snow: Implications for atmospheric iron deposition and algal production in Antarctic waters. *Geophysical Research Letters*, *28*(20), 3907–3910. https://doi.org/10.1029/2001gl012867

Fahrner, D., Lea, J. M., Brough, S., Mair, D. W. F., & Abermann, J. (2021). Linear response of the Greenland ice sheet's tidewater glacier terminus positions to climate. *Journal of Glaciology*, *67*(262), 193–203. https://doi.org/10.1017/jog.2021.13

Ferrari, G. M., & Ferrario, P. (1989). Behavior of Cd, Pb, and Cu in the marine deltaic area of the Po river (north Adriatic sea). *Water, Air, and Soil Pollution*, *43*(3–4), 323–343. https://doi.org/10.1007/BF00279200

Filipek, L. H., Chao, T. T., & Carpenter, R. H. (1981). Factors affecting the partitioning of Cu, Zn, and Pb in boulder coatings and stream sediments in the vicinity of a polymetallic sulfide deposit. *Chemical Geology*, *33*, 45–64. https://doi.org/10.1016/0009-2541(81)90084-X

Fisher, N. S., Teyssié, J.-L., Krishnaswami, S., & Baskaran, M. (1987). Accumulation of Th, Pb, U, and Ra in marine phytoplankton and its geochemical significance. *Limnology and Oceanography*, *32*(1), 131–142. https://doi.org/10.4319/lo.1987.32.1.0131

Gerringa, L. J. A., Rijkenberg, M. J. A., Slagter, H. A., Laan, P., Paffrath, R., Bauch, D., et al. (2021). Dissolved Cd, Co, Cu, Fe, Mn, Ni, and Zn in the Arctic Ocean. *Journal of Geophysical Research: Oceans*, *126*(9), e2021JC017323. https://doi.org/10.1029/2021jc017323

Graeve, M., & Ludwichowski, K.-U. (2017). *Inorganic nutrients measured on water bottle samples from CTD/large volume water-sampler-system during POLARSTERN cruise PS100 (ARK-XXX/2)*. https://doi.org/10.1594/PANGAEA.879197

Graeve, M., Ludwichowski, K.-U., & Krisch, S. (2019). Inorganic nutrients measured on water bottle samples from ultra clean CTD/water sampler-system during POLARSTERN cruise PS100 (ARK-XXX/2), version 2. https://doi.org/10.1594/PANGAEA.905347

Guay, C. K. H., Zhulidov, A. V., Robarts, R. D., Zhulidov, D. A., Gurtovaya, T. Y., Holmes, R. M., & Headley, J. V. (2010). Measurements of Cd, Cu, Pb, and Zn in the lower reaches of major Eurasian Arctic rivers using trace metal clean techniques. *Environmental Pollution*, *158*(2), 624–630. https://doi.org/10.1016/j.envpol.2009.08.039

Guieu, C., Huang, W. W., Martin, J. M., & Yong, Y. Y. (1996). Outflow of trace metals into the Laptev Sea by the Lena river. *Marine Chemistry*, *53*(3–4), 255–267. https://doi.org/10.1016/0304-4203(95)00093-3

Hawkings, J. R., Skidmore, M. L., Wadham, J. L., Priscu, J. C., Morton, P. L., Hatton, J. E., et al. (2020). Enhanced trace element mobilization by Earth's ice sheets. *Proceedings of the National Academy of Sciences of the United States of America*, *117*(50), 31648–31659. https://doi.org/10.1073/pnas.2014378117

Herbert, L. C., Riedinger, N., Michaud, A. B., Laufer, K., Røy, H., Jørgensen, B. B., et al. (2020). Glacial controls on redox-sensitive trace element cycling in Arctic fjord sediments (Spitsbergen, Svalbard). *Geochimica et Cosmochimica Acta*, *271*, 33–60. https://doi.org/10.1016/j.gca.2019.12.005

Homoky, W. B., Severmann, S., McManus, J., Berelson, W. M., Riedel, T. E., Statham, P. J., & Mills, R. A. (2012). Dissolved oxygen and suspended particles regulate the benthic flux of iron from continental margins. *Marine Chemistry*, *134*(135), 59–70. https://doi.org/10.1016/j.marchem.2012.03.003

Hong, S., Candelone, J.-P., Patterson, C. C., & Boutron, C. F. (1994). Greenland ice evidence of hemispheric lead pollution two millennia ago by Greek and Roman civilizations. *Science*, *265*, 1841–1843. https://doi.org/10.1126/science.265.5180.1841

Hudson, B., Overeem, I., McGrath, D., Syvitski, J. P. M., Mikkelsen, A., & Hasholt, B. (2014). MODIS observed increase in duration and spatial extent of sediment plumes in Greenland fjords. *The Cryosphere*, *8*(4), 1161–1176. https://doi.org/10.5194/tc-8-1161-2014

Huhn, O., Hattermann, T., Davis, P. E. D., Dunker, E., Hellmer, H. H., Nicholls, K. W., et al. (2018). Basal melt and freezing rates from first noble gas samples beneath an ice shelf. *Geophysical Research Letters*, *45*(16), 8455–8461. https://doi.org/10.1029/2018GL079706

Huhn, O., Rhein, M., Bulsiewicz, K., & Sültenfuß, J. (2021). Noble gas (He, Ne isotopes) and transient tracer (CFC-11 and CFC-12) measurements from POLARSTERN cruise PS100 (northeast Greenland). https://doi.org/10.1594/PANGAEA.931336

Huhn, O., Rhein, M., Kanzow, T., Schaffer, J., & Sültenfuß, J. (2021). Submarine meltwater from Nioghalvfjerdsbræ (79 north glacier), Northeast Greenland. *Journal of Geophysical Research: Oceans*, *126*(7), e2021JC017224. https://doi.org/10.1029/2021jc017224

Jean-Baptiste, P., Petit, J. R., Lipenkov, V. Y., Raynaud, D., & Barkov, N. I. (2001). Constraints on hydrothermal processes and water exchange in Lake Vostok from helium isotopes. *Nature*, *411*(6836), 460–462. https://doi.org/10.1038/35078045

Joint Research Centre. (2017). Certified reference material BCR–414. Retrieved January 21, 2020, from https://crm.jrc.ec.europa.eu/p/q/bcr+414/BCR-414-PLANKTON-trace-elements/BCR-414

Kalnejais, L. H., Martin, W. R., & Bothner, M. H. (2015). Porewater dynamics of silver, lead and copper in coastal sediments and implications for benthic metal fluxes. *Science of the Total Environment*, *517*, 178–194. https://doi.org/10.1016/j.scitotenv.2015.02.011

Kalnejais, L. H., Martin, W. R., Signell, R. P., & Bothner, M. H. (2007). Role of sediment resuspension in the remobilization of particulate-phase metals from coastal sediments. *Environmental Science and Technology*, *41*(7), 2282–2288. https://doi.org/10.1021/es061770z

Kanzow, T., Von Appen, W.-J., Schaffer, J., Köhn, E., Tsubouchi, T., Wilson, N., et al. (2017). *Physical oceanography measured with ultra clean CTD/watersampler-system during POLARSTERN cruise PS100 (ARK-XXX/2)*. https://doi.org/10.1594/PANGAEA.871030

Kanzow, T., Von Appen, W.-J., Schaffer, J., Köhn, E., Tsubouchi, T., Wilson, N., & Wisotzki, A. (2017). *Physical oceanography measured on water bottle samples from CTD/large volume watersampler-system during POLARSTERN cruise PS100 (ARK-XXX/2)*. https://doi.org/10.1594/PANGAEA.871028

Kelly, A. E., Reuer, M. K., Goodkin, N. F., & Boyle, E. A. (2009). Lead concentrations and isotopes in corals and water near Bermuda, 1780–2000. *Earth and Planetary Science Letters*, *283*(1–4), 93–100. https://doi.org/10.1016/j.epsl.2009.03.045

Kim, I., Kim, G., & Choy, E. J. (2015). The significant inputs of trace elements and rare earth elements from melting glaciers in Antarctic coastal waters. *Polar Research*, *34*, 24289. https://doi.org/10.3402/polar.v34.24289

Kolb, J., Keiding, J. K., Steenfelt, A., Secher, K., Keulen, N., Rosa, D., & Stensgaard, B. M. (2016). Metallogeny of Greenland. *Ore Geology Reviews*, *78*, 493–555. https://doi.org/10.1016/j.oregeorev.2016.03.006

Kragh, K., Monrad Jensen, S., & Fougt, H. (1997). Ore geological studies of the Citronen fjord zinc deposit, North Greenland: Project "Resources of the sedimentary basins of north and east greenland". *Geology of Greenland Survey Bulletin*, *176*, 44–49. https://doi.org/10.34194/ggub.v176.5060

Krisch, S., Browning, T. J., Graeve, M., Ludwichowski, K. U., Lodeiro, P., Hopwood, M. J., et al. (2020). The influence of Arctic Fe and Atlantic fixed N on summertime primary production in Fram Strait, North Greenland Sea. *Scientific Reports*, *1*, 15230. https://doi.org/10.1038/s41598-020-72100-9

Krisch, S., Hopwood, M. J., Roig, S., Gerringa, L. J. A., Middag, R., Rutgers van der Loeff, M. M., et al. (2022). Arctic – Atlantic exchange of the dissolved micronutrients iron, manganese, cobalt, nickel, copper and zinc with a focus on Fram Strait. *Global Biogeochemical Cycles*, *36*, e2021GB007191. https://doi.org/10.1029/2021GB007191

Krisch, S., Hopwood, M. J., Schaffer, J., Al-Hashem, A. A., Höfer, J., Rutgers van der Loeff, M. M., et al. (2021). The 79°N Glacier cavity modulates subglacial iron export to the NE Greenland Shelf. *Nature Communications*, *12*, 3030. https://doi.org/10.1038/s41467-021-23093-0

Krisch, S., Roig, S., Lodeiro, P., Yong, J. C., Herzberg, N., Steffens, T., et al. (2021). *Dissolved trace elements (Fe, Mn, Co, Ni, Cu, Zn, Cd and Pb) measured on water bottle samples from ultra clean CTD/water sampler-system during POLARSTERN cruise PS100/GN05 (ARK-XXX/2)*. https://doi.org/10.1594/PANGAEA.933431

Lara, R. H., Briones, R., Monroy, M. G., Mullet, M., Humbert, B., Dossot, M., et al. (2011). Galena weathering under simulated calcareous soil conditions. *Science of The Total Environment*, *409*(19), 3971–3979. https://doi.org/10.1016/j.scitotenv.2011.06.055

Laukert, G., Frank, M., Bauch, D., Hathorne, E. C., Rabe, B., Von Appen, W. J., et al. (2017). Ocean circulation and freshwater pathways in the Arctic Mediterranean based on a combined Nd isotope, REE and oxygen isotope section across Fram Strait. *Geochimica et Cosmochimica Acta*, *202*, 285–309. https://doi.org/10.1016/j.gca.2016.12.028

Loose, B., & Jenkins, W. J. (2014). The five stable noble gases are sensitive unambiguous tracers of glacial meltwater. *Geophysical Research Letters*, *41*(8), 2835–2841. https://doi.org/10.1002/2013GL058804

Marani, D., Macchi, G., & Pagano, M. (1995). Lead precipitation in the presence of sulphate and carbonate: Testing of thermodynamic predictions. *Water Research*, *29*(4), 1085–1092. https://doi.org/10.1016/0043-1354(94)00232-V

Marsay, C. M., Aguilar-Islas, A., Fitzsimmons, J. N., Hatta, M., Jensen, L. T., John, S. G., et al. (2018). Dissolved and particulate trace elements in late summer Arctic melt ponds. *Marine Chemistry*, *204*, 70–85. https://doi.org/10.1016/j.marchem.2018.06.002

Martino, M., Turner, A., Nimmo, M., & Millward, G. E. (2002). Resuspension, reactivity and recycling of trace metals in the Mersey Estuary, UK. *Marine Chemistry*, *77*(2–3), 171–186. https://doi.org/10.1016/S0304-4203(01)00086-X

McConnell, J. R., & Edwards, R. (2008). Coal burning leaves toxic heavy metal legacy in the Arctic. *Proceedings of the National Academy of Sciences*, *105*(34), 12140–12144. https://doi.org/10.1073/pnas.0803564105

McConnell, J. R., Wilson, A. I., Stohl, A., Arienzo, M. M., Chellman, N. J., Eckhardt, S., et al. (2018). Lead pollution recorded in Greenland ice indicates European emissions tracked plagues, wars, and imperial expansion during Antiquity. *Proceedings of the National Academy of Sciences of the United States of America*, *115*(22), 5726–5731. https://doi.org/10.1073/pnas.1721818115

Mortensen, J., Bendtsen, J., Motyka, R. J., Lennert, K., Truffer, M., Fahnestock, M., & Rysgaard, S. (2013). On the seasonal freshwater stratification in the proximity of fast-flowing tidewater outlet glaciers in a sub-Arctic sill fjord. *Journal of Geophysical Research: Oceans*, *118*(3), 1382–1395. https://doi.org/10.1002/jgrc.20134

Ndungu, K., Zurbrick, C. M., Stammerjohn, S., Severmann, S., Sherrell, R. M., & Flegal, A. R. (2016). Lead sources to the Amundsen Sea, West Antarctica. *Environmental Science and Technology*, *50*, 6233–6239. https://doi.org/10.1021/acs.est.5b05151

Noble, A. E., Echegoyen-Sanz, Y., Boyle, E. A., Ohnemus, D. C., Lam, P. J., Kayser, R., et al. (2015). Dynamic variability of dissolved Pb and Pb isotope composition from the U.S. North Atlantic GEOTRACES transect. *Deep-Sea Research Part II*, *116*, 208–225. https://doi.org/10.1016/j.dsr2.2014.11.011

Pacyna, J. M., & Pacyna, E. G. (2001). An assessment of global and regional emissions of trace metals to the atmosphere from anthropogenic sources worldwide. *Environmental Reviews*, *9*(4), 269–298. https://doi.org/10.1139/er-9-4-269

Rapp, I., Schlosser, C., Rusiecka, D., Gledhill, M., & Achterberg, E. P. (2017). Automated preconcentration of Fe, Zn, Cu, Ni, Cd, Pb, Co, and Mn in seawater with analysis using high-resolution sector field inductively-coupled plasma mass spectrometry. *Analytica Chimica Acta*, *976*, 1–13. https://doi.org/10.1016/j.aca.2017.05.008

Rhein, M., Steinfeldt, R., Huhn, O., Sültenfuß, J., & Breckenfelder, T. (2018). Greenland submarine melt water observed in the Labrador and Irminger Sea. *Geophysical Research Letters*, *45*(19), 10570–10578. https://doi.org/10.1029/2018GL079110

Rignot, E., & Mouginot, J. (2012). Ice flow in Greenland for the international polar year 2008–2009. *Geophysical Research Letters*, *39*(11), L11501. https://doi.org/10.1029/2012GL051634

Rivera-Duarte, I., & Flegal, A. R. (1994). Benthic lead fluxes in San Francisco Bay, California, USA. *Geochimica et Cosmochimica Acta*, *58*(15), 3307–3313. https://doi.org/10.1016/0016-7037(94)90059-0

Rusiecka, D., Gledhill, M., Milne, A., Achterberg, E. P., Annett, A. L., Atkinson, S., et al. (2018). Anthropogenic signatures of lead in the northeast Atlantic. *Geophysical Research Letters*, *45*(6), 2734–2743. https://doi.org/10.1002/2017GL076825

Santana-Casiano, J. M., Gonzalez-Davila, M., Perez-Peña, J., & Millero, F. J. (1995). Pb2+ interactions with the marine phytoplankton Dunaliella tertiolecta. *Marine Chemistry*, *48*(2), 115–129. https://doi.org/10.1016/0304-4203(95)91418-K

Sañudo-Wilhelmy, S. A., & Flegal, A. R. (1994). Temporal variations in lead concentrations and isotopic composition in the southern California Bight. *Geochimica et Cosmochimica Acta*, *58*(15), 3315–3320. https://doi.org/10.1016/0016-7037(94)90060-4

Schaffer, J., Kanzow, T., Von Appen, W. J., Von Albedyll, L., Arndt, J. E., & Roberts, D. H. (2020). Bathymetry constrains ocean heat supply to Greenland's largest glacier tongue. *Nature Geoscience*, *13*(3), 227–231. https://doi.org/10.1038/s41561-019-0529-x

Schaffer, J., Timmermann, R., Erik Arndt, J., Savstrup Kristensen, S., Mayer, C., Morlighem, M., & Steinhage, D. (2016). A global, high-resolution data set of ice sheet topography, cavity geometry, and ocean bathymetry. *Earth System Science Data*, *8*(2), 543–557. https://doi.org/10.5194/essd-8-543-2016

Schaffer, J., Von Appen, W. J., Dodd, P. A., Hofstede, C., Mayer, C., De Steur, L., & Kanzow, T. (2017). Warm water pathways toward Nioghalvfjerdsfjorden Glacier, northeast Greenland. *Journal of Geophysical Research: Oceans*, *122*, 4004–4020. https://doi.org/10.1002/2016JC012462

Schlitzer, R. (2022). Ocean data view. Retrieved from https://odv.awi.de

Schlosser, C., & Garbe-Schönberg, D. (2019). Mechanisms of Pb supply and removal in two remote (sub-) polar ocean regions. *Marine Pollution Bulletin*, *149*, 110659. https://doi.org/10.1016/j.marpolbul.2019.110659

Sherrell, R. M., Boyle, E. A., Falkner, K. K., & Harris, N. R. (2000). Temporal variability of Cd, Pb, and Pb isotope deposition in central Greenland snow. *Geochemistry, Geophysics, Geosystems*, *1*(1). https://doi.org/10.1029/1999gc000007

Sherrell, R. M., Boyle, E. A., & Hamelin, B. (1992). Isotopic equilibration between dissolved and suspended particulate lead in the Atlantic Ocean: Evidence from 210Pb and stable Pb isotopes. *Journal of Geophysical Research*, *97*(92), 11257–11268. https://doi.org/10.1029/92JC00759

Tanaka, N., Takeda, Y., & Tsunogai, S. (1983). Biological effect on removal of Th-234, Po-210 and Pb-210 from surface water in Funka Bay, Japan. *Geochimica et Cosmochimica Acta*, *47*(10), 1783–1790. https://doi.org/10.1016/0016-7037(83)90026-1

Tanguy, V., Waeles, M., Gigault, J., Cabon, J. Y., Quentel, F., & Riso, R. D. (2011). The removal of colloidal lead during estuarine mixing: Seasonal variations and importance of iron oxides and humic substances. *Marine and Freshwater Research*, *62*(4), 329–341. https://doi.org/10.1071/MF10220

Vieira, L. H., Achterberg, E. P., Scholten, J., Beck, A. J., Liebetrau, V., Mills, M. M., & Arrigo, K. R. (2019). Benthic fluxes of trace metals in the Chukchi Sea and their transport into the Arctic Ocean. *Marine Chemistry*, *208*, 43–55. https://doi.org/10.1016/j.marchem.2018.11.001

Waeles, M., Riso, R. D., Maguer, J.-F., Guillaud, J.-F., & Le Corre, P. (2008). On the distribution of dissolved lead in the Loire estuary and the North Biscay continental shelf, France. *Journal of Marine Systems*, *72*, 358–365. https://doi.org/10.1016/j.jmarsys.2007.01.012

Waeles, M., Riso, R. D., & Le Corre, P. (2007). Distribution and seasonal changes of lead in an estuarine system affected by agricultural practices: The Penzé estuary, NW France. *Estuarine, Coastal and Shelf Science*, *74*, 570–578. https://doi.org/10.1016/j.ecss.2007.05.002

Wagener, T., Guieu, C., & Leblond, N. (2010). Effects of dust deposition on iron cycle in the surface Mediterranean Sea: Results from a mesocosm seeding experiment. *Biogeosciences*, *7*(11), 3769–3781. https://doi.org/10.5194/bg-7-3769-2010

Wani, A. L., Ara, A., & Usmani, J. A. (2015). Lead toxicity: A review. *Interdisciplinary Toxicology*, *8*(2), 55–64. https://doi.org/10.1515/intox-2015-0009

Wei, C. L., & Murray, J. W. (1994). The behavior of scavenged isotopes in marine anoxic environments: 210Pb and 210Po in the water column of the Black Sea. *Geochimica et Cosmochimica Acta*, *58*(7), 1795–1811. https://doi.org/10.1016/0016-7037(94)90537-1

Wilson, N., Straneo, F., & Heimbach, P. (2017). Satellite-derived submarine melt rates and mass balance (2011-2015) for Greenland's largest remaining ice tongues. *The Cryosphere*, *11*(6), 2773–2782. https://doi.org/10.5194/tc-11-2773-2017

Wilson, N. J., & Straneo, F. (2015). Water exchange between the continental shelf and the cavity beneath Nioghalvfjerdsbræ (79 North Glacier). *Geophysical Research Letters*, *42*(18), 7648–7654. https://doi.org/10.1002/2015GL064944

Yang, W., Guo, L., Chuang, C., Santschi, P. H., Schumann, D., & Ayranov, M. (2015). Influence of organic matter on the adsorption of 210Pb, 210Po and 7Be and their fractionation on nanoparticles in seawater. *Earth and Planetary Science Letters*, *423*, 193–201. https://doi.org/10.1016/j.epsl.2015.05.007

Young, T. J., Christoffersen, P., Bougamont, M., Tulaczyk, S. M., Hubbard, B., Mankoff, K. D., et al. (2022). Rapid basal melting of the Greenland ice sheet from surface meltwater drainage. *Proceedings of the National Academy of Sciences of the United States of America*, *119*(10), e2116036119. https://doi.org/10.1073/pnas.2116036119

Zimmer, L. A., Asmund, G., Johansen, P., Mortensen, J., & Hansen, B. W. (2011). Pollution from mining in south Greenland: Uptake and release of Pb by blue mussels (Mytilus edulis L.) documented by transplantation experiments. *Polar Biology*, *34*(3), 431–439. https://doi.org/10.1007/s00300-010-0898-5

Zurbrick, C. M., Boyle, E. A., Kayser, R., Reuer, M. K., Wu, J., Planquette, H., et al. (2018). Dissolved Pb and Pb isotopes in the North Atlantic from the GEOVIDE transect (GEOTRACES GA01) and their decadal evolution. *Biogeosciences*, *15*, 4995–5014. https://doi.org/10.5194/bg-2018-29